Characterization of Al_2O_3 Gate Dielectric for Graphene Electronics on Flexible Substrates

Xinxin Yang, Marlene Bonmann, Andrei Vorobiev, Jan Stake
Terahertz and Millimetre Wave Laboratory, Department of Microtechnology and Nanoscience,
Chalmers University of Technology, SE-41296 Gothenburg, Sweden, xinxiny@chalmers.se

***Abstract*—To ensure the high performance of graphene-based field effect transistors (GFETs) on flexible substrates, an uniform and manufacturable dielectric film with good electrical properties is needed. Thus, electrical characterization of the dielectric film on graphene on flexible substrates is very important for the development of flexible electronics based on GFETs. Here, we have fabricated and characterized parallel-plate capacitor test structures consisting of 35 nm thick Al_2O_3 dielectric film and with graphene as bottom electrode on polyethylene terephthalate (PET). It was found that the leakage current density in the Al_2O_3 film is less than 100 μA/cm^2 at 5 V, which allows for applying it as a gate dielectric in GFETs on flexible substrates. The extracted dielectric constant of the Al_2O_3 film is approx. 7.6, which is close to the bulk value and confirms the good quality of the Al_2O_3 film. Analysis indicates that the measured loss tangent, which is up to 0.2, is governed mainly by the dielectric loss in the Al_2O_3 and can be associated with defects from the Al_2O_3 film and the Al_2O_3/graphene interface. Our results will be used in further development of GFETs on flexible substrates.**

***Index Terms*—Graphene, flexible capacitor, dielectric measurement, RF measurement.**

I. Introduction

Graphene, a two-dimensional sheet of carbon atoms arranged in a honeycomb lattice [1], has recently emerged as an interesting material for flexible electronics due to superb electrical properties, combined with chemical stability and mechanical flexibility [2]. Graphene-based field effect transistors (GFETs) are one of the primary components used in electronic circuits, which have developed rapidly in recent years [3]. In particular, GFETs have great potential for flexible and stretchable devices due to their excellent mechanical flexibility [4], opening up a variety of promising applications in flexible electronics [5]. To ensure the high performance of GFETs on flexible substrates, an uniform and manufacturable dielectric film is needed for efficient charge injection into the graphene channel [6] and direct reduction of impurity scattering at the dielectric/graphene interface [7]. Al_2O_3 is a widely used insulating material for gate dielectric, due to its excellent dielectric properties, strong adhesion to many materials, and thermal and chemical stabilities. However, the properties of the Al_2O_3 film on graphene are very sensitive to growth conditions [8]. Thus, techniques to characterize the electrical properties of the dielectric film on graphene on flexible substrates are very important for the development of flexible electronics based on GFETs. To the best of our knowledge, no studies have been reported on this so far. In this work, we have developed Al_2O_3 capacitor test structures with graphene as bottom electrode on flexible substrate with only one step photolithography and characterized the electrical properties of the Al_2O_3 film.

II. Device Model

Top and cross sectional views of a test structure are shown in Fig. 1 (a) and (b). The white region in Fig. 1 (a) is where the top metal is removed. a and b are inner electrode radius and ring radius, respectively. The equivalent circuit of the structure based on the parallel capacitance model [9] is shown in Fig. 1 (c). Since the area of the outer electrode is much larger than that of the inner electrode, the capacitance of the outer capacitor (C_{o}) is much larger than that of inner (C). Similarly, both the parallel leakage resistance (R_{opl}) and the parallel dielectric resistance (R_{opd}) of the outer capacitor are much smaller than that of the inner. Therefore, C_{o}, R_{opl} and R_{opd} are negligible. R_{s} is the series resistance of graphene. To measure R_{s} in the same conditions as the capacitance measurement, we use the same probe to punch through the dielectric, as shown in Fig. 1 (d). This may cause point contact with larger contact resistance, with which we got the maximum value of R_{s}. R_{ipl} is the parallel leakage resistance of the inner capacitor, which can be deduced from the measurement of leakage current. R_{ipd} is the parallel dielectric resistance of the inner capacitor, which is mainly caused by the defects from the Al_2O_3 film and the Al_2O_3/graphene interface [10].

Based on the parallel capacitance model in ref. 9, the loss tangent can be expressed as

$$tan\delta_{\mathrm{tot}} = tan\delta_{\mathrm{s}} + \tan\delta_{\mathrm{ipl}} + \tan\delta_{\mathrm{ipd}} + \tan\delta_{\mathrm{PET}}. \quad (1)$$

where $\tan\delta_{\mathrm{s}} = \omega C R_{\mathrm{s}}$ is the loss tangent of the series resistance, $\tan\delta_{\mathrm{ipl}} = 1/(\omega C R_{\mathrm{ipl}})$ is the loss tangent of the parallel leakage resistance, $\tan\delta_{\mathrm{ipd}} = 1/(\omega C R_{\mathrm{ipd}})$ is the loss tangent of the parallel dielectric resistance and $\tan\delta_{\mathrm{PET}}$ ranging from 1×10^{-4} to 5×10^{-4} is the loss tangent from polyethylene terephthalate (PET) substrate.

III. Device Design and Fabrication

The graphene supplied from Graphenea Company was grown by chemical vapor deposition (CVD) and transferred on PET flexible substrate. The dielectric film was formed by natural oxidation of 3 nm thick Al followed by 30 nm thick Al_2O_3 deposited by e-beam evaporation. The total thickness of Al_2O_3 film (t) is 35 nm. The top electrode layer (Ti/Au

978-1-5090-1348-7/16/$31.00 ©2016 IEEE

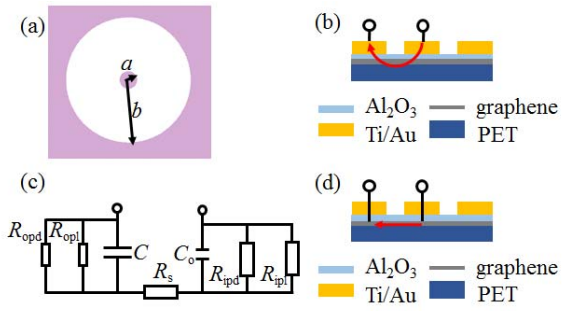

Fig. 1. (a) Top and (b) cross sectional view of the test structure; (c) the equivalent electrical circuit of the test structure; (d) the cross sectional view of the short structure.

5/100 nm) is then patterned into suitable test structures by photolithography evaporation.

The microphoto of the test structures on PET is shown in Fig. 2. The dark ring region on the pattern is where the top metal is lifted off. The difference between the two capacitors is that the left one is with graphene under the dielectric film, while the right one is without. The ripples of the outer electrode on the left can be associated with delamination at graphene/PET interface due to strain caused by the large outer electrode area. The relatively inner electrodes with smaller area remain intact. Our previous results indicate that there is no delamination of GFET structures with typical total dimension within $100 \times 100\ \mu m^2$.

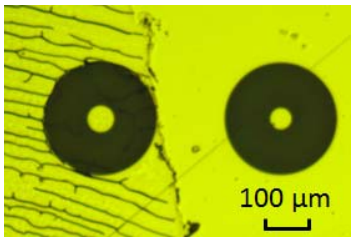

Fig. 2. The microphoto of two test structures.

IV. Experimental Results and Discussions

The leakage current of the test structures is measured using a Keithley 2604B SourceMeter. The capacitance and loss tangent of the test structures are measured using a HP 4285A LCR Meter at 1 MHz frequency.

The leakage current density versus gate voltage of a test structure is shown in Fig. 3. The leakage current is attributed to a combination of tunneling current and charging current. It is less than 100 μA/cm^2 when the gate voltage is 5 V, which is negligible compared to drain current in GFETs and photocurrent in terahertz detectors based on GFETs [11]. The breakdown electric field is about 5 mV/cm, which is similar to reported Al_2O_3 ALD films on silicon [12]. Thus, we can apply the Al_2O_3 as gate dielectric in GFETs on flexible substrates. As the dielectric voltage is swept from negative to positive (-7 V to 7 V) and back (7 V to -7 V), a pronounced hysteresis is observed except for low voltages where the leakage current is determined by the thermal noise current, which is caused by charging current [13].

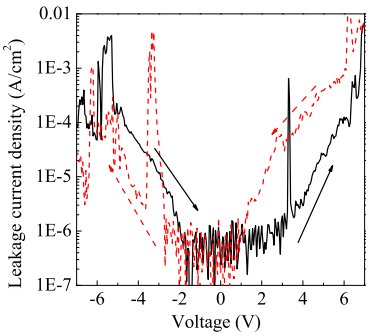

Fig. 3. Leakage current density of a test structure with $a = 25\ \mu$m versus applied voltage. The arrows denote the different sweeping directions.

The measured capacitance versus area of the inner electrode is shown in Fig. 4. The dielectric constant can be calculated from the measured capacitance based on the parallel-plate capacitor model, $\epsilon_r = Ct/\epsilon_0 A$. Here ϵ_r is the dielectric constant of the dielectric film, ϵ_0 is the permittivity of free-space and $A = \pi a^2$ is the area of the inner electrode. The capacitance increases linearly with the increase of inner electrode area while the dielectric constant is stable. The dielectric constant is approx. 7.6, which is sightly less than the bulk Al_2O_3 dielectric constant ranging from 8 to 10 [14]. This may be caused by the series quantum capacitance of graphene, or the deviations of the Al_2O_3 thickness. The result confirms the good quality of the Al_2O_3 dielectric film.

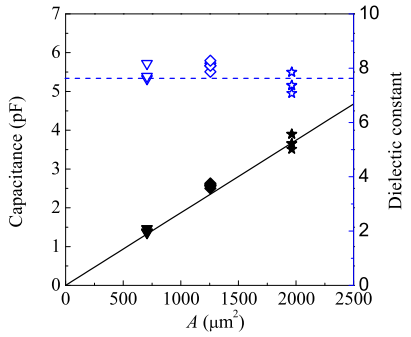

Fig. 4. Capacitance (solid symbols, left axes) and dielectric constant (open symbols, right axes) versus area of the inner electrode. The solid line is modeled capacitance curve with $\epsilon_r = 7.6$. The dash line is $\epsilon_r = 7.6$.

The $\tan\delta_{tot}$ in the gate dielectric of GFETs is correlated to the carrier mobility in graphene. The carrier mobility increases sharply with the decrease of $\tan\delta_{tot}$ [15]. The measured $\tan\delta_{tot}$, simulated $\tan\delta_s$ and $\tan\delta_{ipl}$ versus area of the inner electrode are shown in Fig. 5, in which $\tan\delta_{PET}$ is negligible. $\tan\delta_s$ is calculated with the capacitance density and R_s being 200 pF/cm^2 and 1000 Ω, respectively. Similarly, $\tan\delta_{ipl}$ is calculated when capacitance density is 200 pF/cm^2 and the parallel leakage resistance density is 1×10^5 Ω /cm^2. $\tan\delta_s$

increases with the increase of the inner electrode area, while $\tan\delta_{\rm ipl}$ is constant. However, both $\tan\delta_{\rm s}$ and $\tan\delta_{\rm ipl}$ are much less than $\tan\delta_{\rm tot}$. So $\tan\delta_{\rm tot}$ is governed mainly by the dielectric loss in Al_2O_3 and can be associate with defects from the Al_2O_3 film and the Al_2O_3/graphene interface. Futher optimization of the Al_2O_3 technology may greatly decrease the $\tan\delta_{tot}$ and thus increase the carrier mobility.

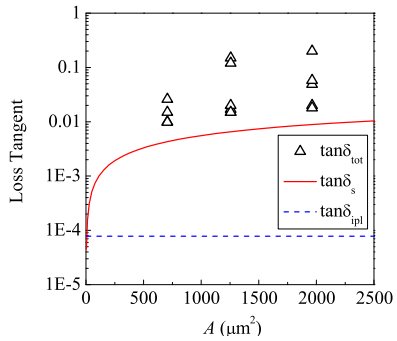

Fig. 5. The measured $\tan\delta_{\rm tot}$ (symbols) and simulated $\tan\delta_{\rm s}$ (solid line) and $\tan\delta_{\rm ipl}$ (dash line) versus area of the inner electrode.

Furthermore, we have fabricated GFETs with Al_2O_3 as gate dielectric with the growth processes as mentioned above on PET substrate. The loss tangent of GFETs was calculated using the reflective coefficient measured by an Agilent N5230A vector network analyzer without drain bias [9]. The measured loss tangent of a GFET versus frequency is shown in Fig. 6. The linear increase of measured loss tangent with the increase in frequency indicates that the series resistance dominates measured loss tangent. The series resistance consists of the access resistance and the metal/graphene contact resistance. Thus, a possible path to improve performance of high frequency GFETs is to reduce the series resistance based on perfecting the design and fabrication process. The series resistance can be extracted from the real part of the measured input impedance [9]. Hence, the corresponding loss tangent of series resistance can be subtracted from the total loss tangent. The de-embedded loss tangent is shown in Fig. 6. As the loss from the PET substrate is negligible, the de-embedded loss tangent represents the dielectric loss in the Al_2O_3 film. The maximum in the frequency dependence of the de-embedded loss tangent can be explained by relaxation of the polarization associated with defects.

V. Conclusion

In conclusion, the electrical properties of Al_2O_3 gate dielectric has been characterized based on parallel-plate capacitor test structures consisting of 35 nm thick Al_2O_3 and graphene as bottom electrode on PET. The results show that the leakage current density in Al_2O_3 is less than 100 μA/cm^2 at 5 V and the dielectric constant of the Al_2O_3 film is approx. 7.6. This confirms the good quality of the dielectric and allows for applying it as a gate dielectric in GFETs on flexible substrates. The loss tangent of the Al_2O_3 film is governed mainly by the loss from defects. Our work will allow better understanding and promote further development of GFETs on flexible substrates.

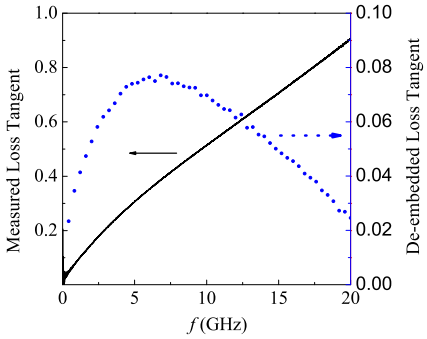

Fig. 6. Measured (solid line, left axes) and de-embedded (dotted line, right axes) loss tangents of a GFET with 1.2 μm gate length versus frequency.

Acknowledgment

This work was supported in part by the EU Graphene Flagship, in part by the Swedish Foundation of Strategic Research (SSF), and in part by the Knut and Alice Wallenberg Foundation (KAW).

References

[1] K. S. Novoselov, A. K. Geim, S. Morozov, D. Jiang, Y. Zhang, S. Dubonos, , I. Grigorieva, and A. Firsov, "Electric field effect in atomically thin carbon films," *Science*, vol. 306, no. 5696, pp. 666–669, 2004.

[2] G. Eda, G. Fanchini, and M. Chhowalla, "Large-area ultrathin films of reduced graphene oxide as a transparent and flexible electronic material," *Nature nanotechnology*, vol. 3, no. 5, pp. 270–274, 2008.

[3] F. Schwierz, "Graphene transistors," *Nature nanotechnology*, vol. 5, no. 7, pp. 487–496, 2010.

[4] B. J. Kim, H. Jang, S.-K. Lee, B. H. Hong, J.-H. Ahn, and J. H. Cho, "High-performance flexible graphene field effect transistors with ion gel gate dielectrics," *Nano letters*, vol. 10, no. 9, pp. 3464–3466, 2010.

[5] Y. Liang, X. Liang, Z. Zhang, W. Li, X. Huo, and L. Peng, "High mobility flexible graphene field-effect transistors and ambipolar radio-frequency circuits," *Nanoscale*, vol. 7, no. 25, pp. 10 954–10 962, 2015.

[6] A. Javey, H. Kim, M. Brink, Q. Wang, A. Ural, J. Guo, P. McIntyre, P. McEuen, M. Lundstrom, and H. Dai, "High-κ dielectrics for advanced carbon-nanotube transistors and logic gates," *Nature materials*, vol. 1, no. 4, pp. 241–246, 2002.

[7] C. Jang, S. Adam, J.-H. Chen, E. Williams, S. D. Sarma, and M. Fuhrer, "Tuning the effective fine structure constant in graphene: opposing effects of dielectric screening on short-and long-range potential scattering," *Physical review letters*, vol. 101, no. 14, p. 146805, 2008.

[8] H. Lin, P. Ye, and G. Wilk, "Leakage current and breakdown electric-field studies on ultrathin atomic-layer-deposited al2o3 on gaas," *Applied physics letters*, vol. 87, no. 18, p. 182904, 2005.

[9] A. Vorobiev, S. Gevorgian, M. Löffler, and E. Olsson, "Correlations between microstructure and q-factor of tunable thin film bulk acoustic wave resonators," *Journal of Applied Physics*, vol. 110, no. 5, p. 054102, 2011.

[10] A. K. Jonscher, *Universal relaxation law: a sequel to Dielectric relaxation in solids*. Chelsea Dielectrics Press, 1996.

[11] L. Vicarelli, M. Vitiello, D. Coquillat, A. Lombardo, A. Ferrari, W. Knap, M. Polini, V. Pellegrini, and A. Tredicucci, "Graphene field-effect transistors as room-temperature terahertz detectors," *Nature materials*, vol. 11, no. 10, pp. 865–871, 2012.

[12] M. Groner, J. Elam, F. Fabreguette, and S. M. George, "Electrical characterization of thin al 2 o 3 films grown by atomic layer deposition on silicon and various metal substrates," *Thin Solid Films*, vol. 413, no. 1, pp. 186–197, 2002.
[13] H. Wang, Y. Wu, C. Cong, J. Shang, and T. Yu, "Hysteresis of electronic transport in graphene transistors," *ACS nano*, vol. 4, no. 12, pp. 7221–7228, 2010.
[14] R. Singh and R. Ulrich, "High and low dielectric constant materials," *Electrochemical Society Interface*, vol. 8, no. 2, pp. 26–30, 1999.
[15] S. Bidmeshkipour, A. Vorobiev, M. Andersson, A. Kompany, and J. Stake, "Effect of ferroelectric substrate on carrier mobility in graphene field-effect transistors," *Applied Physics Letters*, vol. 107, no. 17, p. 173106, 2015.